Journal of the Korean Society for Nondestructive Testing
Vol. 29, No. 3 (2009. 6)

Visualization of Tooth for Non-Destructive Evaluation from CT Images

Hui Gao* and Oksam Chae*†

Abstract This paper reports an effort to develop 3D tooth visualization system from CT sequence images as a part of the non-destructive evaluation suitable for the simulation of endodontics, orthodontics and other dental treatments. We focus on the segmentation and visualization for the individual tooth. In dental CT images teeth are touching the adjacent teeth or surrounded by the alveolar bones with similar intensity. We propose an improved level set method with shape prior to separate a tooth from other teeth as well as the alveolar bones. Reconstructed 3D model of individual tooth based on the segmentation results indicates that our technique is a very conducive tool for tooth visualization, evaluation and diagnosis. Some comparative visualization results validate the non-destructive function of our method.

Keywords: Segmentation, Visualization, Level Set Method, Dental CT Image

1. Introduction

The nondestructive reconstruction of human body parts such as internal organs, bones and teeth becomes an important tool for computer aided diagnosis (CAD) systems in both medical and dental field in recent years. They are essential to evaluate the structure and to plan the treatment of the parts without affecting human body. X-ray dental radiographs are intensively used for tooth restoration and human identification (Nomir and Abdel-Mottaleb, 2005). Range images are also used for the segmentation of dental study models (Kondo et al., 2004). However those images provide limited information for completely understanding the tooth structure. With the development of computerized tomography technique, dental CT images provide much more information for tooth visualization and dental treatment.

In this paper we report a research to develop 3D tooth visualization system from CT sequence images. The system contains three main components: dental CT imaging, image sequence segmentation and 3D tooth visualization. We introduce the two main dental CT imaging modalities and basic visualization techniques. The direct volume rendering method can visualize the whole maxillofacial region, but is difficult to locate and manipulate the region of interest independently such as teeth. The conventional segmentation method can separate the hard tissue from the soft tissue, and create the specific surface for the region of interest. However due to the intensity similarity of tooth and alveolar bone, the existing segmentation and visualization method have difficulty to separate the individual tooth from other tissues (Hosntalab et al., 2008).

Therefore we propose a tooth reconstruction technique that can construct and visualize individual tooth in nondestructive manner for the pre-evaluation of individual tooth structure and

Received: September 30, 2008, Revised: May 8, 2009, Accepted: May 15, 2009. * Department of Computer Engineering, Kyung Hee University, Seochun-ri, Kiheung-eup, Yongin-si, Kyunggi-do, 446-701, Korea, † Corresponding Author: oschae@khu.ac.kr

the treatment planning. We firstly segment the tooth slice by slice using active contour tracking algorithm, and then create the surface model for each individual tooth. These 3D tooth models can be visualized and manipulated independently. Moreover the segmented teeth can be integrated together with the jaws for comparative evaluations.

The next sections will explore the three main components for tooth visualization system. However our focus will be on the individual tooth segmentation and visualization.

2. Dental CT Imaging Modalities

Computerized tomography can be divided into two main categories based on the acquisition X-ray beam geometry: conventional fan beam CT and cone beam CT (Scarfe et al., 2006).

Fan beam CT technology: In fan-beam scanners, an X-ray source and solid-state detector are mounted on a rotating gantry (Fig. 1a). Data are acquired using a narrow fan-shaped X-ray beam transmitted through the patient. The patient is imaged slice by slice, usually in the axial plane, and interpretation of the images is achieved by stacking the slices to obtain multiple 2D representations. The linear array of detector elements used in conventional helical fan-beam CT scanners is actually a multi-detector array. This configuration allows multi-detector CT (MDCT) scanners to acquire up to 64 slices simultaneously, considerably reducing the scanning time compared with single-slice systems and allowing generation of 3D images at substantially lower doses of radiation than single detector fan-beam CT arrays.

Cone beam CT technology (CBCT): CBCT scanners are based on volumetric tomography, using a 2D extended digital array providing an area detector. This is combined with a 3D cone-shaped X-ray beam (Fig. 1b). The cone-beam technique involves a single 360° scan in which the X-ray source and a reciprocating area detector synchronously move around the patient's head, which is stabilized with a head holder. At certain degree intervals, the projection images are acquired. Software programs incorporating sophisticated algorithms such as FBP (Filtered Back Projection) are applied to these projection images to reconstruct the 3D volumetric data set. Cone beam CT provides significant advantages over conventional CT such as rapid scan time and low dose radiation as well as reduced image artifact, etc. Therefore cone beam CT has been more and more widely used for dental diagnosis and treatment recently.

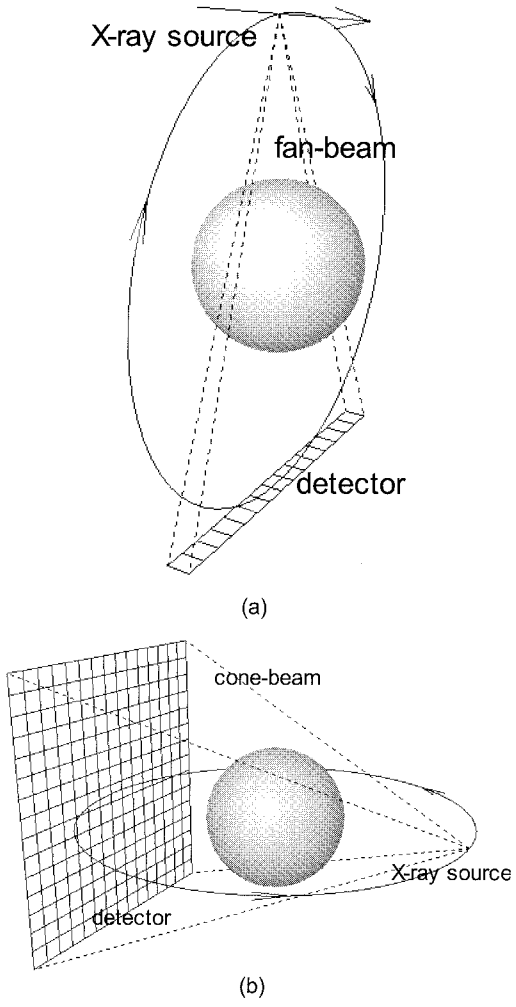

Fig. 1 (a) fan beam dental CT illustration, (b) cone beam dental CT illustration

3. Individual Tooth Segmentation

The overall structure of our 3D dental visualization system from CT images is illustrated in Fig. 2: the source images are generated from the dental CT device. Then individual tooth contours are segmented out from each slice. Next, individual 3D tooth models are constructed from contours. Finally tooth models are integrated with the skull models and used for orthodontic simulations.

The key part for the above system is the individual tooth segmentation. In this section we will propose the active contour tracking method for the tooth segmentation slice by slice. Observe from the slice images that in some middle slices the teeth are free of alveolar bones. These teeth can be easily segmented. However in the slices approaching to the root region, the surrounding alveolar bones have the similar intensity as the teeth, which will ruin most of the normal segmentation methods.

Therefore our basic idea for the proposed algorithm is that: start from one middle slice and segment the contour in this slice. Then the segmented contour is used as the initial contour for the next adjacent slice, and this contour will move to catch the new tooth boundaries. The procedure will be repeated again and again until all the slices have been segmented. As in Fig. 3(a) the starting slice is number 118 and in Fig. 3(b) the starting slice is number 114. The contour in the starting slice is firstly segmented out and then this contour is tracked forward and backward to segment all the slices.

For active contour based tooth segmentation

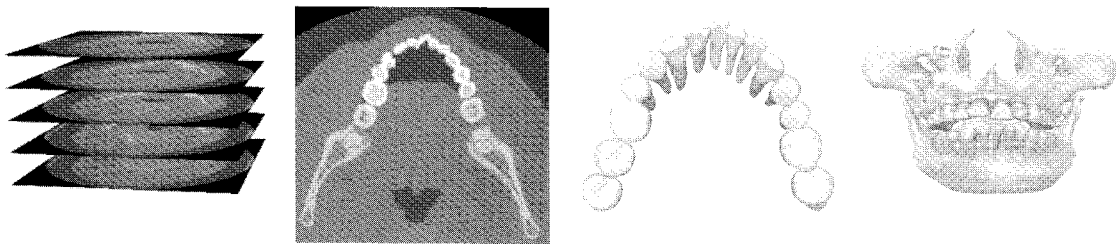

(a) (b) (c) (d)

Fig. 2 (a) CT image slices, (b) individual tooth segmentation result overlapped on the original image, (c) reconstructed 3D tooth models, (d) tooth models rendered together with jaw for orthodontic simulation

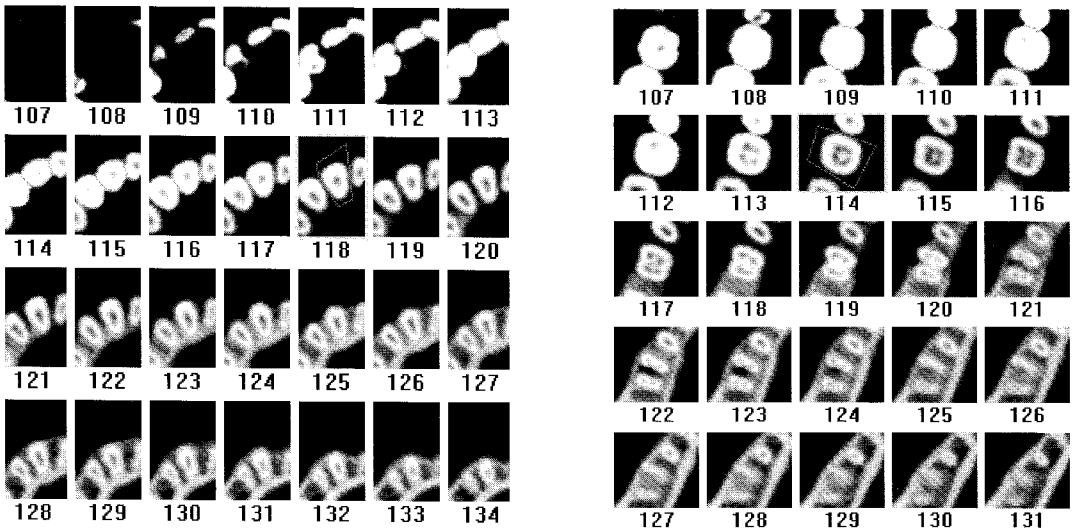

(a) (b)

Fig. 3 Segmentation procedure for a single tooth in consecutive slices

there is one challenging issue, saying, the contour may split from one piece to multiple pieces between the adjacent slices. For molars, from the crown to root the number of the contour used for representing one tooth may vary due to the multiple roots. As illustrated in Fig. 3(b) the contour in slice 120 splits into two pieces in the succeeding slice 121. Usually the tooth contour is represented by control points. However there is no way to relate all the contour points from different contours to one single tooth. Moreover it is difficult to handle the splitting of contour from one piece to multiple pieces. Therefore one uniform method to representing one single contour or multiple contours is required. To this end in the proposed method signed distance function is introduced.

Contour representation (signed distance function): Given an initial contour such as a closed curve C, define the signed distance function ϕ such that in the two-dimensional domain each point has the value which is the minimum distance to this curve from it. For convenience we define that the distance is negative inside the curve and positive outside the curve. So that the curve C can be represented as the set of points which have zero distance values in the signed distance function ϕ. Either one single contour or multiple contours can be represented by one signed distance function.

The given initial contour is not necessary to be exactly on the tooth boundary. It is given approximately close to the desired boundary. Then the signed distance function will deform so that the zero-level contours will move accordingly. Through finding the optimal solution of the signed distance function one can find the optimal solution for contours to segment the desired tooth boundaries.

Contour optimization (level set method): The level set method is an extension to the traditional active contour models (Malladi et al., 1995). It is used for the optimization of the signed distance function. An energy function for level set method was proposed so that the signed distance function which gives the minimal value of this energy function will be the optimum solution (Li et al., 2005):

$$\begin{aligned} E = \mu \int_{\Omega} \frac{1}{2}\left(|\nabla\phi| - 1\right)^2 dxdy + \\ \lambda \int_{\Omega} g\delta(\phi)|\nabla\phi| dxdy + \\ \nu \int_{\Omega} gH(-\phi) dxdy \end{aligned} \tag{1}$$

where $\mu > 0$, $\lambda > 0$, and ν is a signed weight coefficient, Ω is the 2D image domain, δ is the univariate Dirac function, and H is the Heaviside function. g is an edge-detector which can be defined as a positive and decreasing function in terms of the image gradient for our energy minimization problem. The signed distance function is active and deforming to approach the optimum solution. The first term of above formula acts as the internal energy to penalize the deviation of ϕ from a signed distance function during its deformation. The second term makes the contour smooth. The third term makes the contour either shrink or expand depending on the sign of ν. If $\nu > 0$, the contour shrinks, whereas if $\nu < 0$ it expands. For the convergence condition, it will stop at the object boundaries. The evolution equation of ϕ with respect to time t is as following:

$$\begin{aligned} \frac{\partial\phi}{\partial t} = \mu\left[\Delta\phi - \mathrm{div}\left(\frac{\nabla\phi}{|\nabla\phi|}\right)\right] + \\ \delta(\phi)\left(\lambda \mathrm{div}\left(g\frac{\nabla\phi}{|\nabla\phi|}\right) + \nu g\right) \end{aligned} \tag{2}$$

For the proposed method, only the initial contour in the starting slice needs to be specified. It can be put either completely inside the tooth or outside the tooth. Then a fixed coefficient ν can apply. The succeeding slice other than the starting slice will use the segmentation result from the previous slice as the initial contour. However some parts of the contour are inside the current tooth region, whereas some are not. Therefore adaptive coefficient ν should be applied. Either positive or negative ν may be possible. To this end the intensity from the

previous slice is used as the prior to drive the contour move in the current slice, and the adaptive coefficient is set as:

$$v = \log\left(\frac{p_B(I(x,y))}{p_A(I(x,y))}\right) \quad (3)$$

$p_B(I(x,y))$ is the a prior probability that the image intensity belongs to the background and $p_A(I(x,y))$ is the a prior probability that the image intensity belongs to the object. We can get the probability model from the previous slice. The intuitive understanding about it is that the low intensity region is more likely to be the background which implies that $p_B(I(x,y))$ is greater than $p_A(I(x,y))$. If the initial contour lies on this region then it will shrink and move inward to the interface of the background and the object. Whereas the high intensity region is more likely to be the object which implies that $p_B(I(x,y))$ is less than $p_A(I(x,y))$. If the initial contour lies on this region then it will expand and move outward to the interface of the background and the object. Finally it will stop on the new boundary between background and object.

Driven by the adaptive shrinking or expanding force, all the tooth contours throughout all the slices can be tracked correctly. Moreover thanks to the capability of the signed distance function to automatically handling the contour splitting, all the tooth roots can be detected efficiently.

4. 3D Visualization

Surface rendering: 3D visualization from the geometry elements pre-extracted from the volumetric data is called surface rendering. In our method, the geometry elements are tooth contours segmented from different slices. Surface rendering techniques eliminate the internal structures and only keep the surface information. The surfaces are comprised of triangle or quadrilateral meshes. The meshes are rendered by different color and shading (Jones and Chen, 1994). The surface models can be manipulated independently which is a significant advantage for tooth movement simulation in the orthodontic treatment planning.

Direct volume rendering: Direct volume rendering does not use intermediate geometrical representations, in contrast to surface rendering techniques (Kruger and Westermann, 2003). It offers the possibility for displaying weak or fuzzy surfaces. This frees one from the requirement to make a decision whether a surface is present or not. Suppose a ray is shot into the data volume from the desired point of view, at evenly spaced locations along the ray, the voxel intensity is mapped to certain color and opacity values with predefined transfer functions. The interpolated colors and opacities are merged with each other and with the background by compositing in back-to-front order to yield the color of the final pixel. All the composite pixels are projected onto the 2D viewing plane and displayed in the screen. An opacity value of 0 means totally transparent and a value of 1 means totally opaque. A big advantage of direct volume rendering is that the interior information is not thrown away and can be displayed in the translucent style, so that it enables one to look at the 3D dataset as a whole.

Due to the respective advantages of surface rendering and direct volume rendering, we will present visualization results based on both methods in next section. The comparative results will validate the non-destructive function of our proposed method.

5. Experimental Results

We present some of the results to demonstrate the capability of our method for handling different image conditions. We tested both fan beam and cone beam CT datasets. The fan beam dataset has the slice thickness of 0.63 mm and pixel spacing of 0.4 mm×0.4 mm. The cone beam dataset has the slice thickness of 0.3 mm and pixel spacing of 0.3 mm×0.3 mm.

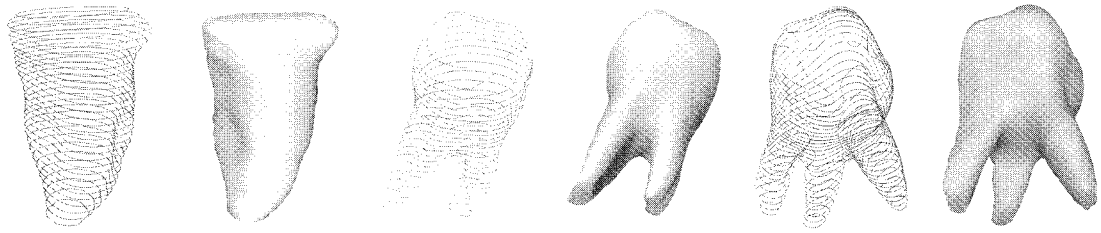

(a) (b) (c) (d) (e) (f)

Fig. 4 Both contours and the rendered 3D models for tooth with one root (a), (b), two roots (c), (d) and three roots (e), (f)

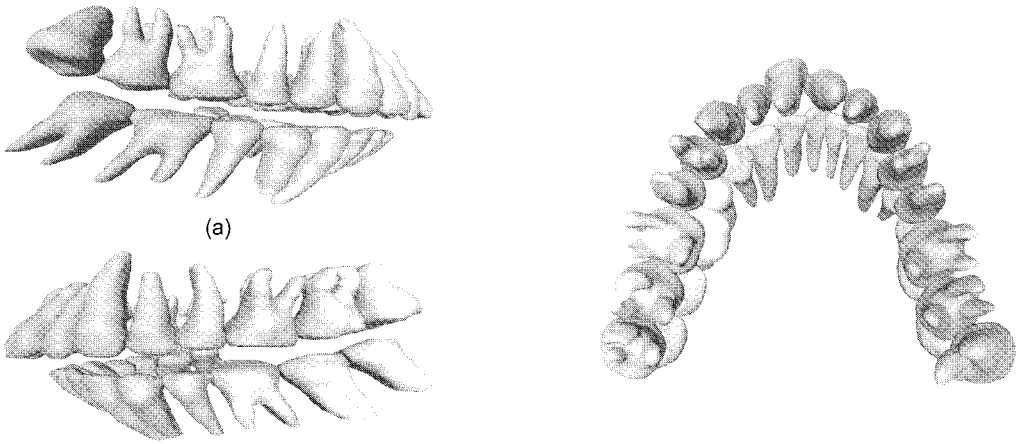

(a) (b) (c)

Fig. 5 Different views of the whole 3D dentition display

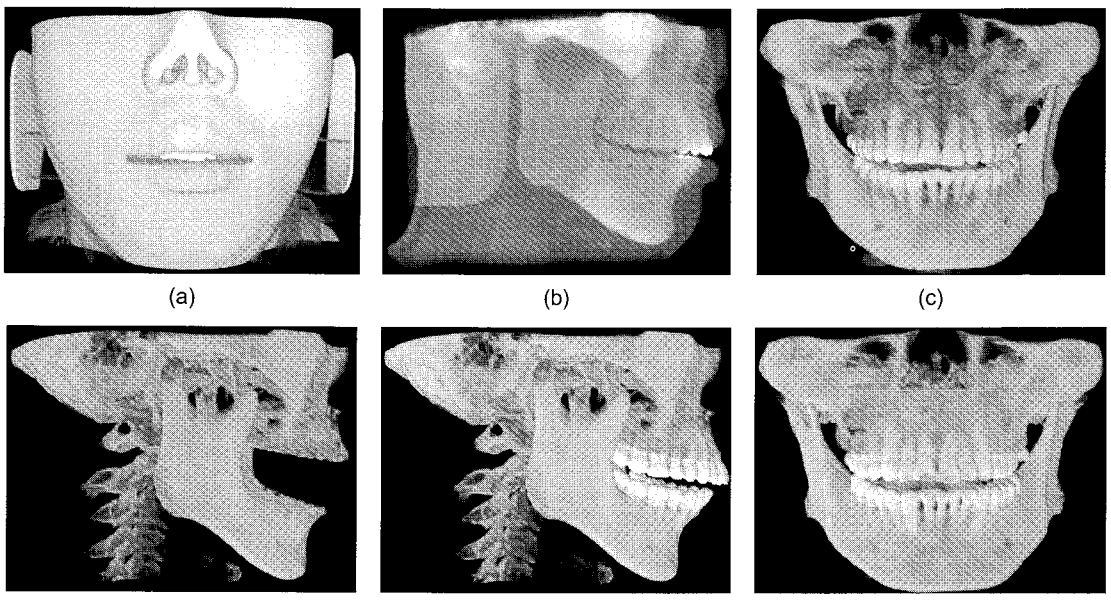

(a) (b) (c)

(d) (e) (f)

Fig. 6 (a), (b), (c) volume rendering for dentomaxillofacial region with different opacity. (d), (e), (f) segmented teeth are displayed together with the jaw

Fan beam dental CT images are less noisy, but the inter-slice resolution is low. Cone beam CT images are noisier, but the inter-slice resolution is relatively high. The proposed method works well for both types of dataset.

We present three individual teeth for 3D surface modeling illustration: one canine, one molar with two roots and one molar with three roots. Both the contours and the rendered 3D models are depicted in Fig. 4. We also present the whole 3D dentition displayed from different views in Fig. 5.

We explored the direct volume rendering techniques as well. Fig. 6(a), (b), (c) show the dentomaxillofacial region. With different opacity the interior structures are also visible. We also integrate segmented teeth together with the jaw (Fig. 6(d), (e)). Thanks to the segmentation the teeth are distinguished from the jaw even they have the similar intensity. With only direct volume rendering the teeth cannot be distin- guished from the jaw. Difference between two visualization methods can be observed from Fig. 6(c) and (f).

6. Discussion and Conclusions

The proposed method presents a novel level set method with shape prior to segment tooth contours for 3D visualization from CT images. It segments the teeth from bones and separates the individual tooth from the adjacent teeth successfully. The proposed visualization technique is nondestructive which can be used in various dental treatments plan or simulation.

Although the computation is expensive for the FBP algorithm, level set method and direct volume rendering method, GPU (Graphical Processing Units) can be used to accelerate the computation significantly (Kruger and Westermann, 2003). All the computations for the segmentation and visualization can be done within a few minutes. Our future work is to provide further assistant diagnosis for dental diseases such as tooth lesion, cleft palate and interproximal caries based on our segmentation and visualization results.

References

Hosntalab, M., Zoroofi, R. A., Tehrani-Fard, A. A. and Shirani, Gh. (2008) Segmentation of Teeth in CT Volumetric Dataset by Panoramic Projection and Variational Level Set, *Int. J. CARS,* Vol. 3, pp. 257-265

Jones, M. W. and Chen, M. (1994) A New Approach to the Construction of Surfaces from Contour Data, *Eurographics,* Vol. 13, No. 3, pp. 75-84

Kondo, T., Ong, S. H. and Foong, K. W. C. (2004) Tooth Segmentation of Dental Study Models Using Range Images, *IEEE Trans. on Medical Imaging,* Vol. 23, pp. 350-362

Kruger, J. and Westermann, R. (2003) Acceleration Techniques for GPU-Based Volume Rendering, *Proceedings of the 14th IEEE Visualization Conference,* pp. 287-292

Li, C., Xu, C., Gui, C. and Fox, M. D. (2005) Level Set Evolution without Re-Initialization: A New Variational Formulation, *Proc. IEEE Conference on Computer Vision and Pattern Recognition,* pp. 430-436

Malladi, R., Sethian, J. A. and Vemuri, B. C. (1995) Shape Modeling with front Propagation: A Level Set Approach, *IEEE Trans. Patt. Anal. Mach. Intell,* Vol. 17, pp. 158-175

Nomir, O. and Abdel-Mottaleb, M. (2005) A System for Human Identification from X-ray Dental Rradiographs, *Pattern Recognition,* Vol. 38, pp. 1295-1305

Scarfe, W. C., Farman, A. G. and Sukovic, P. (2006) Clinical Applications of Cone-Beam Computed Tomography in Dental Practice, *J. Can. Dent. Assoc.,* Vol. 72, No. 1, pp. 75-80